

FLUX EXPULSION STUDIES OF NIOBIUM MATERIAL FOR 650 MHz CAVITIES FOR PIP-II

K. McGee, G. Wu, F. Furuta, M. Martinello, O. Melnychuk, A. Netepenko, Y. Xie
Fermilab, Batavia, IL, USA

Abstract

Two different vendors supplied the niobium sheet material for prototype and pre-production PIP-II 5-cell 650 MHz cavities, of both low- β ($\beta = 0.61$) and high- β ($\beta = 0.92$) types. The ASTM sizes of this sheet material were found to differ both by lot and by manufacturer. These cavities were then heat-treated at various temperatures, and their flux expulsion performance was measured. Cavities fabricated from Vendor O material initially trapped most magnetic flux despite being cooled through a high thermal gradient, however, 900°C heat treatment subsequently improved the flux expulsion to an acceptable level. In contrast, Vendor A materials expelled flux very well initially, and 900°C annealing imparted no significant improvement. Understanding and characterizing these materials' flux expulsion properties and responses to heat treatment in detail will be critical to upcoming projects employing these two vendors' niobium.

INTRODUCTION

The Proton Improvement Plan-II (PIP-II) linear accelerator under development at Fermilab (FNAL) is a continuous-wave (CW)-compatible machine, which necessitates the usage of superconducting niobium cavities with field-leading quality factors (Q_0) [1]. Advanced RF surface processing techniques such as N-doping [2] and furnace-baking [3] have been explored mostly in the context of 1.3 GHz TESLA-type cavities, delivering very high quality factors. In the case of N-doping, the strength of these results lead to the industrialization of the technique for application in the Linear Coherent Light Source-II (LCLS-II) production cavities [4].

The PIP-II specifications for Q_0 in their 650 MHz cavities ($Q_0 = 2.4 \times 10^{10}$ at 15.9 MV/m for the $\beta = 0.61$ cavities and $Q_0 = 3.3 \times 10^{10}$ at 17.8 MV/m $\beta = 0.92$) have motivated study of the adaptation of these advanced RF surface processing techniques to lower frequency ranges, with promising initial results [5,6]. Unfortunately, while both recipes can produce cavities with very high Q_0 , they also significantly increase a cavity's sensitivity to trapped magnetic flux.

Magnetic flux sensitivity, S , is a measure of the increase in cavity RF surface resistance per unit of trapped flux, measured in n Ω /mG. Even in a low-Gauss environment, cavities can be expected to experience a few mG of background field, and with measured N-doping and furnace baking sensitivities being on the order of 3-4 n Ω /mG, the temperature-independent RF surface resistance arising from flux trapping can easily become the dominant contribution to the cavity's total RF surface resistance, and thus the primary Q_0 -limiting factor.

It is thus desirable to keep flux trapping in these cavities to an absolute minimum. While it is always practical to use active and passive magnetic shielding techniques in vertical test dewars, or passive shielding and good magnetic hygiene practices in cryomodules, to minimize the presence of trappable magnetic flux in the first place, it is still useful to study the means by which whatever residual field escapes these measures can be expelled from the cavities most efficiently during cooldown.

It has been shown that increasing the spatial cooldown gradient can promote flux expulsion [7], however practical experience has shown that this technique is not equally effective across all cavities [8]. Previous studies have shown that the ability of the cavity to expel magnetic flux does not correlate with grain size [9], but could be more strongly related to the dislocation density, increased during the coldworking processes, which can be unique to vendor, or even lot, of niobium [10].

Thus, when approaching a production project such as PIP-II, it is critical to understand in detail the specific flux expulsion properties of the niobium from the vendor with which the project intends to work. Moreover, one must also understand the treatments most likely to produce the best flux-expelling results so that they may be planned for, and implemented in production runs.

NIOBIUM SOURCES

Prototype and pre-production versions of the $\beta = 0.61$ and $\beta = 0.92$ 650 MHz 5-cell elliptical cavities were fabricated from niobium material from two different vendors, whom we shall refer to as "Vendor A" and "Vendor O." Table 1 lists each of these vendors, subdivided by niobium lot, and ASTM measurements.

Table 1: Niobium Material Sources

Niobium version	ASTM size	Hardness (HV10)	Elongation (%)	Specification	Notes
Vendor O v1	~7	≤ 60	≥ 30	XFEL	Used in LCLS-II
Vendor O v2	~6	≤ 60	≥ 30	XFEL	Used in PIP-II LB650 prototype (EZ-001, EZ-002, and 1-cell)
Vendor O v3	~5	≤ 50	≥ 50	PIP-II	Used in PIP-II LB650 Pre-production
Vendor O v4	~4.5	≤ 50	≥ 50	PIP-II	Used in LB650 Pre-production
Vendor A	~5	≤ 50	≥ 50	PIP-II	Used in PIP-II HB650 prototype

CAVITY FLUX EXPULSION SIMULATION

In order to quantify the flux expulsion properties of the cavities the cryomodule and vertical testing contexts, magnetic field strength measurements are taken with fluxgate magnetic probes mounted at the cavity equators before

(B_{nc}) and after (B_{sc}) the superconducting transition. The ratio B_{sc}/B_{nc} is the “flux expulsion ratio,” which we seek to maximise.

The ideal maximum for this ratio for each cavity’s geometry can be found by means of simulation. The COMSOL results from modelling the ideal flux expulsion ratio for both $\beta = 0.61$ and $\beta = 0.92$ 650 MHz 5-cell elliptical cavity geometries are shown in Figure 1. Note the areas of stronger expulsion around the equator regions, which is where the fluxgate magnetic probes are placed.

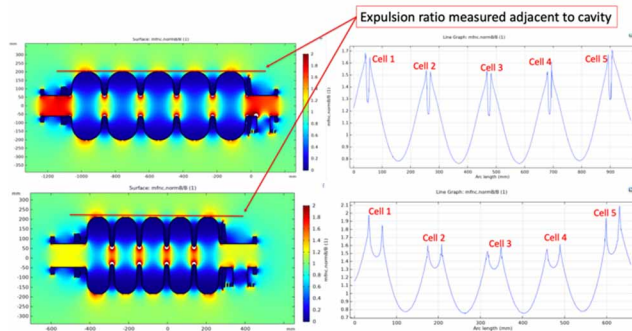


Figure 1, Left: Ideal flux expulsion (B_{sc}/B_{nc}) simulated for a 650 MHz niobium cavity, showing the flux expulsion ratios as a heatmap. Right: Value of B_{sc}/B_{nc} plotted as a function of linear distance along the outer edge of the cavity, as indicated by the red lines.

EXPERIMENTAL SETUP

Cavity Preparation

After receipt from the vendors, all cavities underwent 120 μm bulk electropolishing (EP), followed by 3 h of either 800°C or 900°C vacuum furnace baking. The cavities were then tuned, after which they received a final 40 μm of EP, where the final 20 μm was conducted as “Cold EP,” around (12°C). No further chemistry or heat treatments were conducted after this point. The cavities were then high-pressure water-rinsed (HPR) with DI water before clean assembly to the vertical test insert and hardware.

Vertical Testing

All cavities underwent testing at the FNAL vertical test stand. Cavity instrumentation specific to the flux expulsion measurement consisted of fluxgate magnetic probes affixed to cavity cell equators #1 and #4, with two additional temperature sensors (RTDs) associated with each: one attached at the equator next to the fluxgate probe, and the other attached at the iris above that equator. RTDs positioned in this manner allow for the quantification of the thermal gradient ($\Delta T/dx$) as:

$$\frac{\Delta T}{dx} = \frac{T_{iris} - T_{equator}}{dx},$$

where T_{iris} is taken the moment $T_{equator}$ reaches 9.2 K, and dx is the linear distance between the RTDs at the equator and iris. In the course of FNAL VTS preparation, Helmholtz coils are typically installed around the cavity as a means of actively compensating the ambient magnetic field

during cooldown. In flux expulsion experiments such as the ones conducted herein, these were instead used to impose ~ 100 mG of magnetic field on the cavity during cooldown. Figure 2 shows a representative example of cell #1 of a 5-cell $\beta = 0.92$ 650 MHz cavity instrumented in this way.

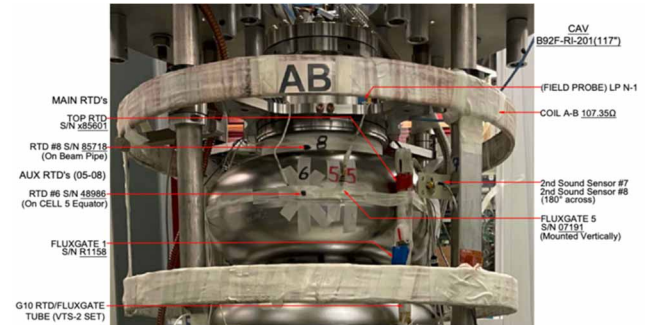


Figure 2: Example cavity instrumentation setup for flux expulsion measurement in the Fermilab vertical test stand.

Thermocycling a cavity to perform a full flux expulsion measurement involves bringing the cavity up to various temperatures, imposing a DC magnetic field of ~ 100 mG, then cooling them again through the superconducting transition temperature, T_c . Varying the peak temperatures to which the cavity is warmed before cooling again allows for different thermal gradients to be tested for their effect on flux expulsion.

RESULTS

The results of the flux expulsion measurements are shown in Figures 3 for the two 5-cell $\beta = 0.92$ 650 MHz cavities tested, fabricated from Vendor A material, and in Figure 4 for the two 5-cell $\beta = 0.61$ 650 MHz cavities, fabricated from Vendor O material.

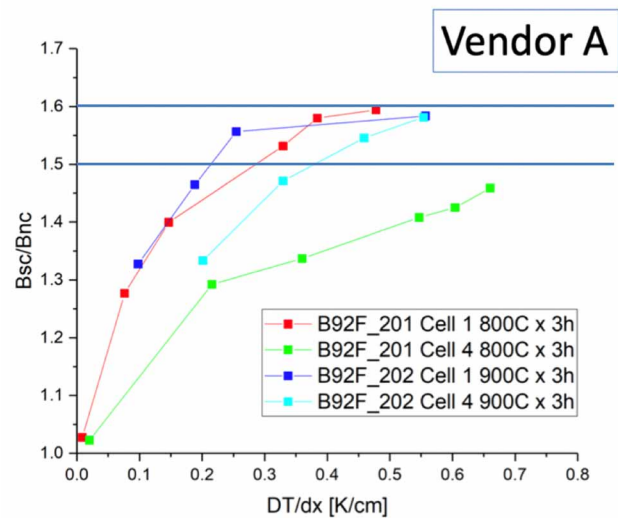


Figure 3: Flux expulsion ratio (B_{sc}/B_{nc}) measured as a function of thermal gradient (DT/dx) for 5-cell $\beta = 0.92$ 650 MHz cavities fabricated from Vendor A material. Both 800 °C and 900 °C materials have flux expulsion ratios close to their simulated ideal levels.

Content from this work may be used under the terms of the CC BY 4.0 licence (© 2023). Any distribution of this work must maintain attribution to the author(s), title of the work, publisher, and DOI

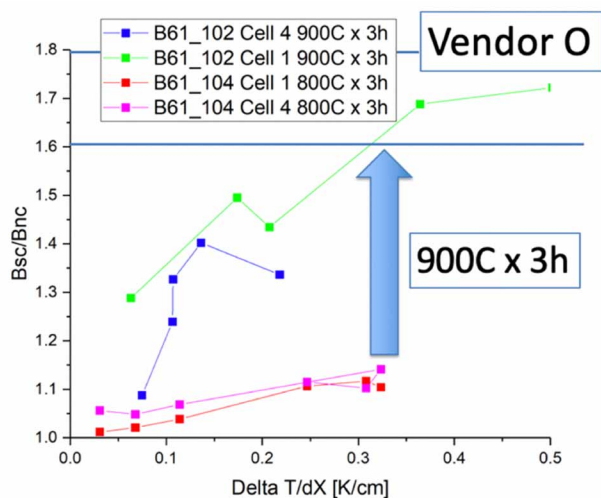


Figure 4: Flux expulsion ratio (B_{sc}/B_{nc}) measured as a function of thermal gradient (DT/dx) for 5-cell $\beta = 0.61$ 650 MHz cavities fabricated from Vendor O material. 800 °C treated cavities expelled flux relatively poorly, whereas 900 °C cavities have flux expulsion ratios close to their simulated ideal levels.

The 5-cell $\beta = 0.92$ cavities shown Figure 3 each had Cell #1 and Cell #4 instrumented for flux expulsion measurements. The simulation results in Figure 1 show that complete expulsion around Cell #1 results in a B_{sc}/B_{nc} of approximately 1.6, and complete expulsion around Cell #4 results in a B_{sc}/B_{nc} of approximately 1.5, and the experimental measurements of these B_{sc}/B_{nc} values came very close to these ideals, as can be seen by comparison between the measurement points and the line overlays. This implies that the Vendor A material does not need 900 °C annealing to reach satisfactory flux expulsion levels.

Avoiding the 900 °C baking treatment where possible is desirable because the additional high-temperature annealing has the potential to detrimentally soften the niobium cavities, making them more prone to de-tuning, which is concerning in the context of cavity transport, or even general handling.

As in the 5-cell $\beta = 0.92$ cavity trials, the 5-cell $\beta = 0.61$ cavity trials shown Figure 4 also had both Cell #1 and Cell #4 instrumented for flux expulsion measurements. However, unlike the Vendor A material, the cavities fabricated from Vendor O material expelled flux quite poorly after 800 °C x 3 h baking, but showed a strong improvement in flux expulsion after the 900 °C x 3 h baking.

DISCUSSION

Cavities fabricated from Vendor A material expelled flux well without the need for higher-temperature treatment, which is attractive for applications in which maintaining structural integrity of the cavities is of concern. Cavity designs with steep sidewall angles, for example, such as the $\beta = 0.61$ 650 MHz cavities, may benefit from construction of such material, since maintaining mechanical stiffness is already a challenge due to the cavity's inherent shape.

Cavities fabricated from Vendor O material likely will require 900 °C annealing before their flux expulsion performance can reach acceptable levels. This suggests that Vendor O material is more appropriate for cavities with somewhat more robust shapes, such as the $\beta = 0.92$ 650 MHz cavities.

Good magnetic hygiene practices are the first defense against magnetic flux trapping, and successful background flux mitigation can obviate the need for fast cooldowns and cavities that expel flux well. However, it remains prudent to explore the flux expulsion properties of various niobium materials so that it is understood to what extent cavity performance can be rescued in the event that flux is indeed trapped in the cryomodules.

CONCLUSIONS

Cavities fabricated from Vendor A material expelled flux well without the need for higher-temperature treatment, whereas cavities fabricated from Vendor O materials required 900 °C annealing before they expelled flux well. This suggests future projects may wish to consider fabricating cavities with inherently less stiff geometries such as the $\beta = 0.61$ 650 MHz cavities out of Vendor A material, in order to avoid 900 °C annealing. Cavities destined to be fabricated out of Vendor O material, conversely, should plan on including 900 °C annealing as part of the production processing.

ACKNOWLEDGEMENTS

This document was prepared using the resources of the Fermi National Accelerator Laboratory (Fermilab), a U.S. Department of Energy, Office of Science, HEP User Facility. Fermilab is managed by Fermi Research Alliance, LLC (FRA), acting under Contract No. DE-AC02-07CH11359.

REFERENCES

- [1] M. Ball *et al.*, "The PIP-II Conceptual Design Report", 2017. <https://lss.fnal.gov/archive/design/fermilab-design-2017-01.pdf>
- [2] A. Grassellino *et al.*, "Nitrogen and argon doping of niobium for superconducting radio frequency cavities: a pathway to highly efficient accelerating structures", *Supercond. Sci. Technol.*, vol. 26, p. 102001, 2013. doi:10.1088/0953-2048/26/10/102001
- [3] H. Ito, H. Araki, K. Takahashi, and K. Umemori, "Influence of furnace baking on Q-E behavior of superconducting accelerating cavities", *Prog Theor. Exp. Phys.*, p. 071G01, 2021. doi:10.1093/ptep/ptab056
- [4] D. Gonnella *et al.*, "Industrialization of the nitrogen-doping preparation for SRF cavities for LCLS-II", *Nucl. Instrum. Methods Phys. Res., Sect. A*, vol. 883, 2018. doi:10.1016/j.nima.2017.11.047
- [5] M. Martinello *et al.*, "Q-factor optimization for high-beta 650 MHz cavities for PIP-II", *J. Appl. Phys.*, vol. 130, p. 174501, 2021. doi:10.1063/5.0068531
- [6] K. McGee *et al.*, "Medium-Velocity Superconducting Cavity for High Accelerating Gradient Continuous-Wave Hadron Linear Accelerators", *Phys. Rev. Accel. Beams*, vol. 24,

p. 112003, 2021.
doi:10.1103/PhysRevAccelBeams.24.112003

[7] A. Romanenko *et al.*, “Dependence of the residual surface resistance of superconducting radio frequency cavities on the cooling dynamics around T_c ”, *J. Appl. Phys.*, vol. 115, p. 184903, 2014. doi:10.1063/1.4875655

[8] S. Posen *et al.*, “Efficient expulsion of magnetic flux in superconducting radio frequency cavities for high Q_0 applications”, *J. Appl. Phys.*, vol. 119, p. 213903, 2016. doi:10.1063/1.4953087

[9] K. McGee *et al.*, “Flux expulsion and material properties of Nb explored in ~650 MHz cavities”, in *Proc IPAC'23*, Venice, Italy, May 2023, paper WEPA157, to be published.

[10] Z. L. Thune, C. McKinney, N. G. Fleming, and T. R. Bieler, “The Influence of Strain Path and Heat Treatment Variations on Recrystallization in Cold-Rolled High-Purity Niobium Polycrystals”, *IEEE Trans. Appl. Supercond.*, vol. 33, no. 5, pp. 1–4, Aug. 2023. doi:10.1109/TASC.2023.324853